https://dx.doi.org/10.1016/j.jclepro.2017.10.005


# Synthesis of zeolite A using sewage sludge ash for application in warm mix asphalt

Yuan Zhang, Zhen Leng*, Fuliao Zou, Lei Wang, Season S. Chen, Daniel C.W. Tsang
Department of Civil and Environmental Engineering, The Hong Kong Polytechnic University, Hung Hom, Kowloon, Hong Kong
*Corresponding author. Email address: zhen.leng@polyu.edu.hk

**Abstract**: Conventional landfill disposal of Sewage Sludge Ash (SSA) generates increasing environmental and economic concerns. This study aims to develop an innovative measure to solve this waste disposal problem by means of synthesizing zeolite A from the SSA and using it as a Warm Mix Asphalt (WMA) additive, which can decrease the construction temperature of asphalt pavement, thus reducing the associated energy consumption and pollutant emission. Alkaline fusion followed by hydrothermal reaction was implemented to synthesize zeolite A from the SSA. The orthogonal experimental design was carried out to optimize the synthesis conditions. The synthetic products were characterized using a Thermogravimetry-Differential Thermal Analyzer (TG-DTA), an X-ray Diffractometer (XRD) and a Scanning Electron Microscope (SEM). The zeolite product synthesized under the optimized conditions showed a desirable thermal property of gradual release of crystalline water up to 18.5% when heated to 200 ºC. Its XRD spectrum validated the presence of zeolite A with high purity. The SSA-derived zeolite A was then used as a WMA additive to produce asphalt mixture at lower construction temperatures, which proved to reduce the construction temperatures of asphalt mixture by 25 ºC. The approach to use SSA-derived zeolite can decline the environmental and economic burden and it can be a cleaner production method of WMA additive for environmental benefits.

**Keywords**: sewage sludge ash, zeolite A, alkaline fusion, hydrothermal reaction, warm mix asphalt

## 1. Introduction

The disposal of sewage sludge and its incineration ash at landfills generates increasing environmental and economic concerns in Hong Kong and many other urban cities with high population density (Lam et al., 2016). According to the latest waste statistics published by the

Hong Kong Environmental Protection Department, on average per day, 801 tons of dewatered sewage sludge from sewage treatment plants was treated by incineration for energy recovery and volume reduction, leaving only the residue and ash with approximately 63 wt% reduction, which was disposed of at landfills (HK EPD, 2017). However, the sewage sludge ash (SSA) is still of huge amount (approximately 296 tons per day) and presents unavoidable environmental and economic burden.

Various options have been investigated for the purpose of beneficial resource recovery from the SSA. For instance, the utilization of the SSA for the fabrication of mortar and concrete was evaluated as an alternative technique in developing sustainable construction materials and waste management (Cyr et al., 2007; Smol et al., 2015). The beneficial use of iron components of the SSA in ceramic materials (Tang and Shih, 2014) and the recovery of phosphorus from the SSA (Cieslik and Konieczka, 2017) were possibly feasible options as well. In this study, the SSA was used to synthesize zeolite A and the SSA-derived zeolite A was applied as a WMA additive in the asphalt mixture.

The concept of WMA is an emerging and green paving technology, which allows asphalt pavements to be constructed at lower temperatures compared to the conventional hot mix asphalt (HMA) pavements without compromising their engineering performance (Al-Qadi et al., 2012). It was proven that WMA is able to significantly save energy consumption and reduce $CO_2$ emissions during asphalt pavement construction (Vidal et al., 2013; Rodriguez-Alloza et al., 2015). The temperature reduction achieved by WMA comes from the use of various approaches in the following three groups: organic additives (Sanche-Alonso et al., 2011), chemical additives (Leng et al., 2013), and water-based or water-containing foaming processes (Rubio et al., 2012; Stimilli et al., 2017).

In the water-containing foaming process, zeolite additives are added to the asphalt mixture because zeolites are microporous hydrated aluminosilicates which contain crystalline water. At high construction temperatures, the crystalline water in zeolites will be released and vaporized, creating volume expansion or foaming of asphalt binder and thus improving its workability and aggregate coating at lower temperatures (Hurley and Prowell, 2005; Topal et al., 2014). Currently, both commercial synthetic zeolites (e.g., Aspha-Min®) (Hossain et al., 2009) and natural zeolite (e.g. clinoptilolite) (Sengoz et al., 2013; Dubravský and Mandula, 2015) are used as WMA additives.

Zeolite additives can provide a viable tool for reducing mixing and compaction temperatures without affecting the basic engineering properties of asphalt mixtures.

It is interesting to note that synthetic zeolites may be produced from waste materials such as coal fly ash (Cardoso et al., 2015; Kim and Lee, 2009), which is obviously more economically and environmentally viable than commercial products synthesized from chemical reagents. The zeolite synthesis from loam minerals and waste materials containing Si and Al sources (e.g. kaolin and fly ash) by the hydrothermal reaction consists of three steps (Rios et al., 2009; Murayama et al., 2002): the dissolution step of Si and Al, the condensation step of silicate and aluminate ions in alkali solution to make aluminosilicate gel, and the crystallization step of aluminosilicate gel to make zeolite crystal. Zeolite A can gradually release its crystalline water between 100 ºC to 200 ºC, Which is found the most suitable for applying as a WMA additive (Afzal et al., 2000; Woszuk and Franus, 2017).

In this research, the SSA was used to synthesize zeolite A and serve as a WMA additive, which is a novel waste management and cleaner production strategy. The TG-DTA, XRD, and SEM were performed to characterize the SSA-derived zeolite A. Afterwards, WMA mixture was produced with the SSA-derived A and measured for the basic engineering properties.

## 2. Experimental program and testing methodologies

### *2.1. Materials*

The SSA was obtained from a sludge treatment facility (T-Park) in Tuen Mun of Hong Kong, where dewatered sewage sludge from sewage treatment plants was treated by incineration for energy recovery and volume reduction, leaving only the residue and ash for landfill disposal (HK EPD, 2017). The chemical compositions of the obtained SSA were determined by X-ray fluorescence (XRF) analysis. Table 1 presents its chemical compositions in a form of major oxides at weight percentages. The SSA contains 33.89% $SiO_2$ and 14.77% $Al_2O_3$, which are major source materials providing the Si and Al for synthesis of zeolite. The crystalline phases of the obtained SSA were determined by X-ray Diffractometer (XRD) analysis. Figure 1 shows the XRD analysis results, from which the following three major crystalline phases can be detected: quartz ($SiO_2$), magnetite ($Fe_2O_3$), and anorthoclase ($(Na,K)Al{\cdot}Si_3O_8$).

Table 1 XRF result of SSA illustrating the quantities (wt %) of major oxides.

| Oxides | $SiO_2$ | $Fe_2O_3$ | $Al_2O_3$ | $P_2O_5$ | CaO | $Na_2O$ | $SO_3$ | $K_2O$ | MgO | ZnO | $TiO_2$ |
|---|---|---|---|---|---|---|---|---|---|---|---|
| [%] | 33.89 | 16.49 | 14.77 | 9.33 | 7.49 | 6.99 | 3.67 | 2.89 | 2.62 | 0.46 | 0.46 |

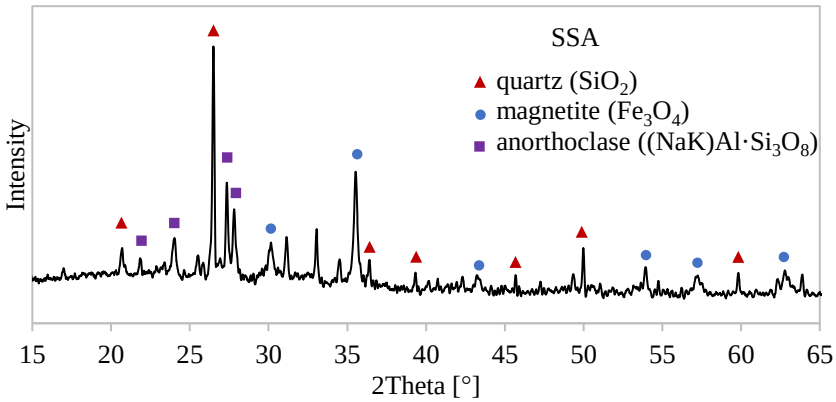


Fig. 1. XRD pattern of SSA illustrating the major crystalline phases.

*2.2. Synthesis process*

Figure 2 illustrates the flow chat of the synthesis process used in this research. The synthesis process comprises two stages: alkaline fusion and hydrothermal reaction. In the alkaline fusion process, the SSA was ground and mixed with the sodium hydroxide (NaOH) powder to obtain a homogeneous mixture. Then, the mixture was heated in a ceramic crucible in air at 500 ºC for 1 h. It was reported that the alkaline fusion with a mass ratio of NaOH and fly ash around 1.2 could convert the insoluble fly ash mineral phase to soluble sodium aluminosilicate phase (Molina and Poole, 2004; Musyoka et al., 2012). The SSA has quartz as the main crystalline mineral phase which is similar to the fly ashes. In order to explore the influence of NaOH on the fused products, different mass ratios of NaOH and SSA (from 0.8 to 1.25) were used in this research. The XRD analysis was performed on the fused products to detect the change of the insoluble crystalline phases, for instance, the conversion of quartz to silicates, in order to determine the appropriate mass ratio of NaOH and SSA for alkaline fusion.

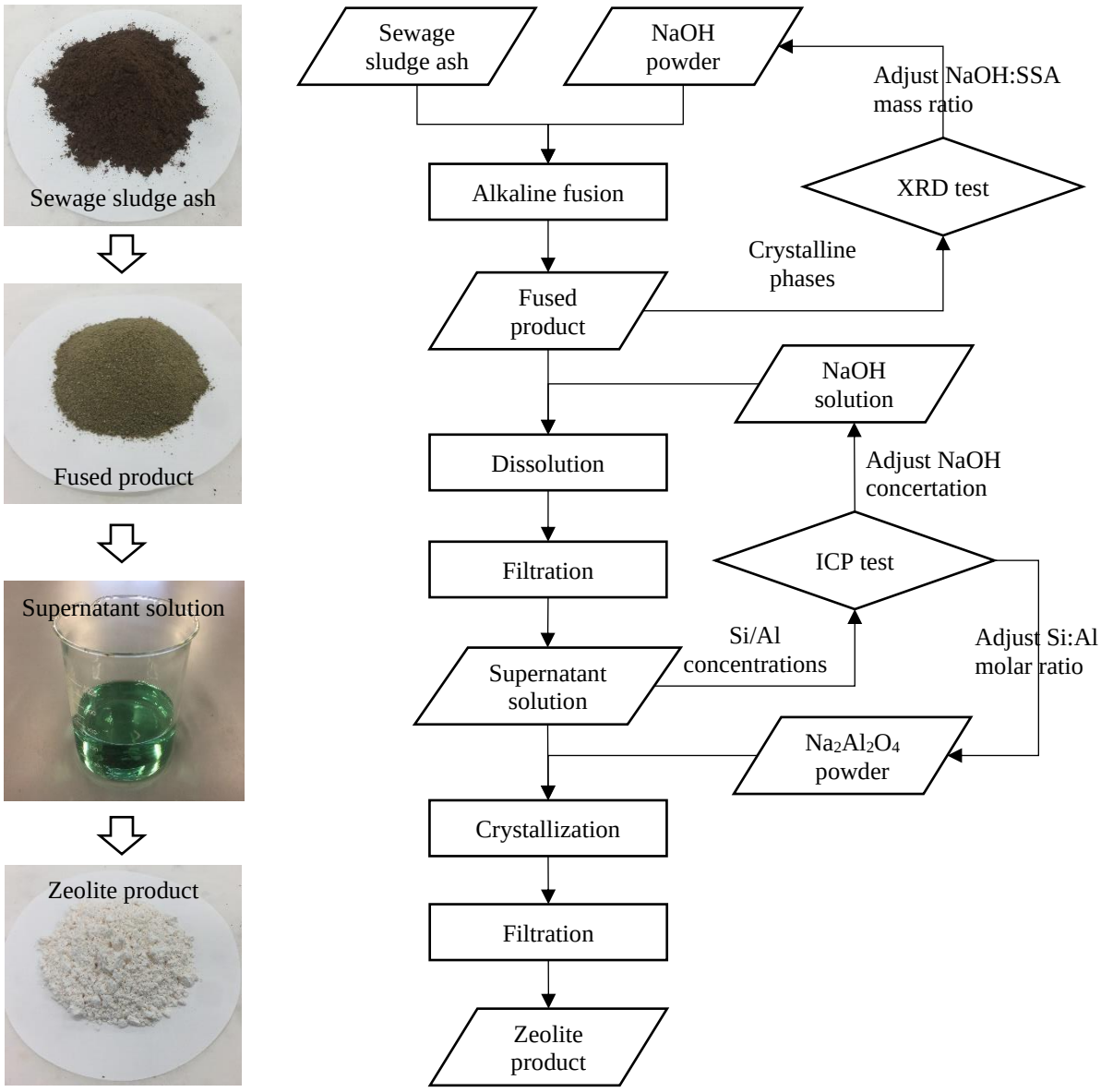


Fig. 2. Flow chat of the synthesis process.

In the hydrothermal reaction process, the first 10 g fused product was mixed with 100 ml NaOH solution. The slurry was stirred for 3 h with a magnetic stirrer at 65 ºC to allow dissolution of the Si and Al from the fused product into the NaOH solution. The slurry was then filtered to acquire clear solution for the crystallization stage. Different NaOH concentrations (from 0 to 3 mol/L) were used to investigate its influence on the clear solution. The Inductively Coupled Plasma-Optical Emission Spectroscopy (ICP-OES) analysis was carried out to measure the Si and Al concentrations in the supernatant solution. Afterwards, the sodium aluminate ($Na_2Al_2O_4$) powder

was added to the supernatant solution to adjust the molar ratio of Si and Al for forming crystallization gel. The resultant crystallization gel was then transferred into a Teflon™ reaction vessel for crystallization of zeolite.

The crystallization conditions were optimized by means of the design of experiments using the Taguchi method (Rao et al., 2008). The L9 orthogonal array of the Taguchi method was chosen to select a subset of the combinations of variables. Three main influential factors were taken into consideration: Si/Al molar ratio, crystallization temperature, and reaction time. The Si/Al molar ratio primarily determines the types of the synthetic zeolites and their resultant physical properties. The rate of crystallization is directly proportional to temperature while the rate of nucleation is inversely proportional to temperature. The reaction time should be adjusted to minimize the production of other phases while obtaining the desired crystalline phase (Georgiev et al., 2009; Bukhari et al., 2015). For each of these factors, three levels were selected. The Si/Al molar ratios (0.75-0.85) were chosen since it was reported that zeolite A is preferable to form at a Si/Al molar ratio around 0.8 (Hollman et al., 1999; Tanaka et al., 2008). Table 2 gives the orthogonal array and experimental parameters in the design of experiments. Nine experimental runs were conducted to synthesis zeolite product. After the hydrothermal reaction, the Teflon™ reaction vessel was transferred to a large container with water at room temperature for cooling down quickly. The synthetic products were then separated by filtration, washed repeatedly with distilled water and then dried over night at 60 ºC. Target zeolite product was produced from the optimal synthesis conditions and used as WMA additive in the subsequent experiments.

Table 2 Orthogonal array and experimental parameters in the design of experiments.

| Experiment | Parameters | | | Sample code |
|---|---|---|---|---|
| | Si/Al molar ratio [-] | Crystallization temperature [ºC] | Reaction time [h] | |
| 1 | 0.75 | 80 | 3 | S-1 |
| 2 | 0.75 | 90 | 6 | S-2 |
| 3 | 0.75 | 100 | 9 | S-3 |
| 4 | 0.80 | 80 | 6 | S-4 |
| 5 | 0.80 | 90 | 9 | S-5 |
| 6 | 0.80 | 100 | 3 | S-6 |
| 7 | 0.85 | 80 | 9 | S-7 |
| 8 | 0.85 | 90 | 3 | S-8 |
| 9 | 0.85 | 100 | 6 | S-9 |

In the Taguchi method, the Signal-to-Noise (S/N) ratios are recommended for selecting the best combination of design variables (Joseph and Pignatiello, 1988). The best design is one which maximizes the S/N ratio. When the responses are non-negative and the larger values are considered to be better, the S/N ratio recommended by Taguchi is described as following equation:

$$Z(x_j) = -10\log\left(\frac{1}{n}\sum_{i=1}^{n}\left(1/y_{ji}\right)^2\right)$$

where $x_j$ represents the factor x at level j, n is the number of experimental runs, and $y_{ji}$ denotes the measured response of samples from the factor x at j level.

*2.3. SSA-derived zeolite characterization*

The thermal properties of the synthetic products were observed through the TG-DTA analysis using a Rigaka Thermo plus EVO2 thermal analyzer with a TG resolution of 0.1 µg. The synthetic products were heated in air from ambient temperature to 600 ºC at a fixed heating rate of 10 ºC/min. The XRD analysis was employed to determine the crystalline phases of the synthetic products. A Rigaku SmartLab X-ray diffractometer with a high-intensity 9 kW rotating anode X-ray generator which can generate a maximum voltage of 45 kV and a maximum current of 200 mA with Cu target was used. The allowable 2theta scanning range is between -3 degree and 160 degree. The minimum scanning step width is 0.0001 degree. In the XRD tests, the detector was scanned at a step width of 0.02 degree and a scan speed of 4 degree/min. The crystalline phases present in the synthetic products were identified using Rigaku's PDXL software by comparing the detected XRD patterns with the standard patterns from the powder diffraction file database supplied by the International Centre for Diffraction Data (ICDD). The morphology of the synthetic products was investigated by SEM using a Tescan VEGA3 system operating which has a best resolution of 2 nm at 30 kV in high-vacuum mode ($<9\times10^{-3}$ $Pa^2$). The magnification continuous from 3× to 1000000×. The maximum field of view is 7.7 mm at a Working Distance (WD) of 10 mm.

*2.4. Preparation of warm mix asphalt mixtures*

The zeolite product synthesized under the optimal conditions was used as a WMA additive to produce WMA mixture. An HMA mixture was designed and produced as a reference. The mixture

composition used in this research is presented in Table 3, which is the typical 10 mm wearing course asphalt mixture widely applied on highways in Hong Kong. The coarse aggregates, as well as fine aggregates and mineral filler, were from local granite rocks. The used binder was grade 60/70 pen bitumen. The Marshall method was implemented to design the HMA mixture and prepare the specimens. The mineral aggregates and bitumen were heated to temperatures of 165 ºC and 150 ºC, respectively. The compaction temperature for HMA mixture was 145 ºC.

With an addition of WMA additives, WMA mixtures were produced using the same mixture composition and preparation procedure as those for the HMA mixture. The producing and compaction temperatures for WMA mixtures were all reduced by 25 ºC compared to the HMA mixture to evaluate the effects of the zeolite additives on the workability of the bituminous mixture. Two WMA additives (the SSA-derived zeolite and Aspha-Min®) were used to produce WMA mixtures using the same procedure. The commercial WMA additive Aspha-Min® was provided by the Eurovia Services GmbH, which has been investigated in laboratory and applied in test sections (Hossain et al., 2009). The recommended dosage of Aspha-Min® is 0.3% by total weight of the asphalt mixture. This rate was used for the SSA-derived zeolite for comparison. The void contents of HMA and WMA specimens were measured according to the ASTM D3203 (ASTM, 2011). Their Marshall stabilities and flow numbers were measured according to the ASTM D6927 (ASTM, 2015).

Table 3 Mixture composition of the 10 mm wearing course asphalt mixture.

| Components | B.S. Sieve size [mm] | Passing percentage [%] | Apparent density [g/cm$^3$] |
|---|---|---|---|
| Coarse aggregates | 14 | 100 | 2.642 |
| | 10 | 94.0 | 2.663 |
| | 5 | 68.0 | 2.709 |
| Fine aggregates | 2.36 | 51.0 | 2.649 |
| | 1.18 | 34.4 | |
| | 0.6 | 22.6 | |
| | 0.3 | 14.5 | |
| | 0.15 | 9.2 | |
| Mineral filler | 0.075 | 6.0 | 2.661 |
| Binder content [%] | 6.0 (as percentage of total mass including binder) | | |

## 3. Results and discussion

### *3.1. Effect of alkaline fusion*

The major crystalline phase, quartz ($SiO_2$), can be the source material of the Si for synthesizing zeolite. However, quartz is a type of mineral phase which hardly dissolves in solution. The alkaline fusion process was conducted to convert quartz to silicates. The mass ratio of NaOH and SSA for the alkaline fusion varied from 0.8 to 1.25, with a step width of 0.05. Figure 3 shows the XRD patterns of the fused products from different mass ratios of NaOH and SSA. It is obvious that the quantity of quartz decreased with the increasing of mass ratio of NaOH and SSA, as a result of conversion to silicates (Figure 3). When a ratio of 0.85 was used, only a small amount of quartz was converted to silicates. Two groups of silicates were formed in the fused products: olivine and pyroxene minerals. The olivine minerals are nesosilicates in which the silicate tetrahedra are isolated. Attraction between the silicate tetrahedra and positive ions holds minerals of this structure together. The pyroxene minerals are inosilicates which have interlocking chains of silicate tetrahedra. The silicate tetrahedra in this structure link to form a chain by sharing two oxygen atoms each. Both olivine and pyroxene minerals are soluble silicates. When the NaOH/SSA mass ratio reached 1.15, most of the quartz was converted (Figure 3). This ratio is close to the findings of the alkaline fusion on fly ashes for zeolite synthesis (Somerset et al., 2005; Musyoka et al., 2012). It was found that when a higher amount of NaOH powder was used, the fused product was slightly agglutinated. In order to maximize the conversion of quartz and avoid agglutination, the NaOH/SSA mass ratio of 1.15 was chosen for the alkaline fusion.

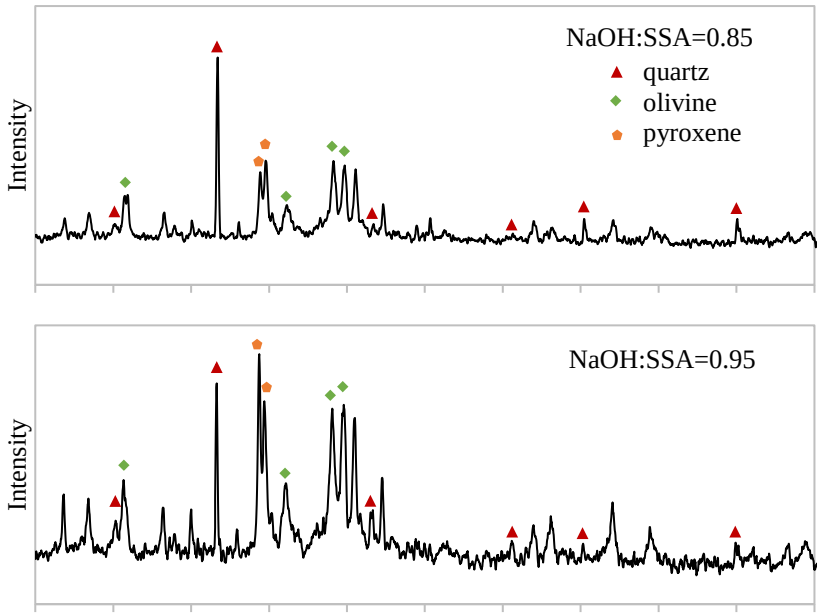

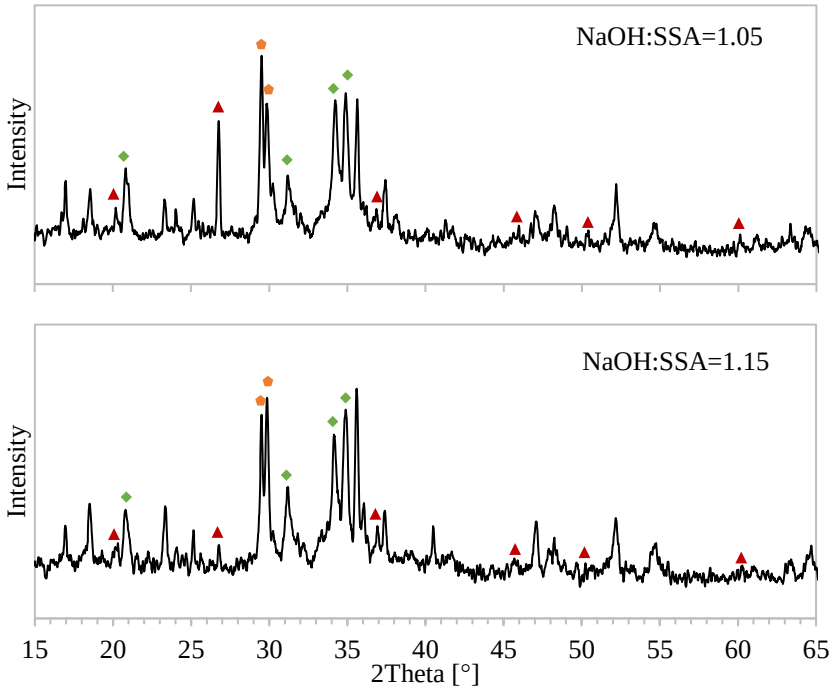


Fig. 3. XRD patterns of the fused products.

*3.2. Influence of NaOH concentration*

For the hydrothermal reaction, the source materials of Si and Al in the fused product need to dissolve in a solution. When 10 g of fused product was added into 100 ml distilled water for dissolution, the Si and Al concentrations in the resultant solution were 4404.4 mg/L and 324.7 mg/L, respectively. As the concentration of NaOH solution increased, more Si and Al dissolved in the solution (Figure 4). Inada et al. (2005) and Latosińska (2016) reported that an appropriate amount of NaOH was needed to accelerate the dissolution of Si and Al from the fly ash. When the NaOH concentration was lower than 2.0 M, the amount of synthetic product was small because of limited dissolution of Si and Al. With a NaOH concentration of 2.5 mol/L, the dissolved Si and Al concentrations reached the maximum values of 6838.4 mg/L and 1434.2 mg/L, respectively. The dissolved percentages of the Si and Al were calculated regarding to their total amounts in the SSA by mass balance, which increased from 56.9% to 86.0%, and from 8.5% to 36.5%, respectively. When the NaOH concentration was increased from 0 to 2.5 mol/L.

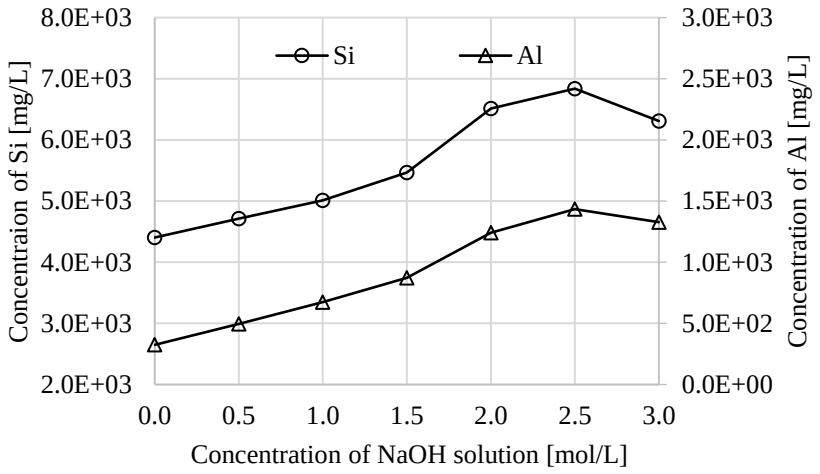


Fig. 4. Dissolved Si and Al concentrations in the solution.

*3.3. Thermal behavior of the synthetic products*

The design of experiments using the Taguchi method was conducted to determine the significance of factors and the optimal parameters. The mass of total water release, which was calculated through multiplying the percentage of water loss and yield of the synthetic product, was taken as the response for analyzing the results from the experimental design. Table 4 presents the responses of the synthetic products, in which the percentage of water loss was obtained by measuring the mass loss of the synthetic product when heated up to 200 ºC.

Table 4 Responses of the synthetic products.

| Specimen code | Percentage of water loss [%] | Yield of synthetic product [g] | Mass of total water release [g] |
|---|---|---|---|
| S-1 | 18.30 | 2.6959 | 0.4933 |
| S-2 | 15.09 | 3.0761 | 0.4643 |
| S-3 | 6.48 | 3.0784 | 0.1995 |
| S-4 | 17.2 | 2.7032 | 0.4653 |
| S-5 | 12.47 | 2.4760 | 0.3087 |
| S-6 | 16.11 | 2.4424 | 0.3936 |
| S-7 | 17.03 | 2.8334 | 0.4825 |
| S-8 | 18.16 | 2.3989 | 0.4356 |
| S-9 | 7.16 | 2.6917 | 0.1928 |

Table 5 presents the results of S/N ratio for the responses of the synthetic products. The higher value of the S/N ratio corresponds to the better performance, which is the higher value of mass of

total water release. The optimal crystallization conditions are at the Si/Al molar ratio of 0.80, crystallization temperature of 80 ºC and reaction time of 3 h. The significance of each factor can be measured using the delta values of the S/N ratios, which is the mathematical range of S/N ratios between all levels for a given factor, i.e., the difference between the maximum and minimum S/N ratios for a given factor. It can be concluded that the effect of crystallization temperature on the response of the synthetic products is more significant, while the Si/Al molar ratio has less influence compared to the other two factors. Figure 5 illustrates the responses of the synthetic products in terms of crystallization temperature and reaction time. When the Si/Al molar ratio is in the range of 0.75 to 0.85, the lower the crystallization temperature, the higher the amount of water released from the synthetic product. The similar trend was found for the reaction time.

Table 5 S/N ratio for the response of synthetic products

| Si/Al molar ratio (-) | | | Crystallization temperature (ºC) | | | Reaction time (h) | | |
|---|---|---|---|---|---|---|---|---|
| Level | | S/N ratio | Level | | S/N ratio | Level | | S/N ratio |
| j=1 | 0.75 | -10.5 | j=1 | 80 | -6.4 | j=1 | 3 | -7.2 |
| j=2 | 0.80 | -8.6 | j=2 | 90 | -8.3 | j=2 | 6 | -10.8 |
| j=3 | 0.85 | -10.8 | j=3 | 100 | -12.9 | j=3 | 9 | -11.2 |
| Delta | | 2.2 | Delta | | 6.5 | Delta | | 4.0 |

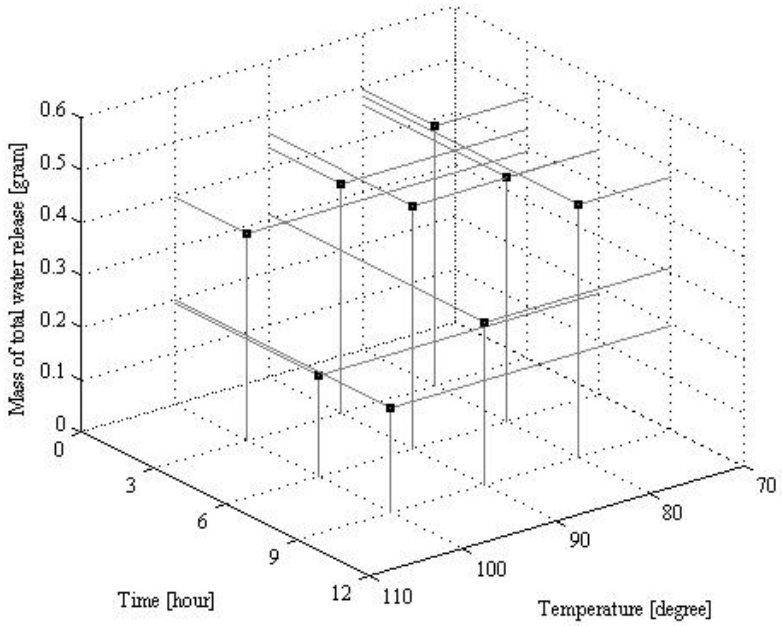


Fig. 5. Responses of synthetic products in terms of crystallization temperature and reaction time.

Under the optimal crystallization conditions, 10 g of fused product obtained 3.035 g synthetic product after the hydrothermal reaction. Figure 6 shows the thermal behavior of this synthetic product, which had an obvious mass loss (from 3.5% to 18.5%) from 70 ºC to 200 ºC. The DTA peak appeared at the temperature of 137 ºC. This synthetic product showed a similar thermal behavior as the zeolite A measured by Afzal et al. (2000) and Musyoka et al. (2015). The percentage of mass loss in this temperature range identified the percentage of crystalline water in this synthetic zeolite and DTA peak suggested its maximum reaction rate due to the release of crystalline water, respectively.

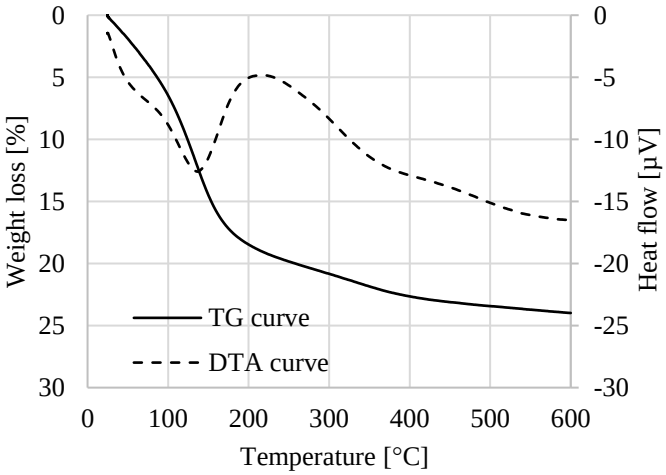


Fig. 6. Thermal behavior of the product synthesized under optimal crystallization conditions.

*3.4. XRD characterization of synthetic products*

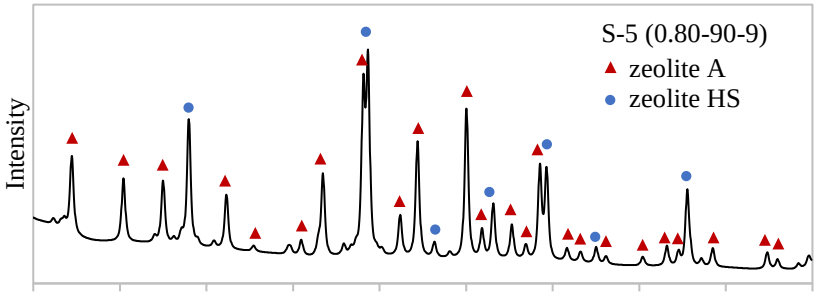

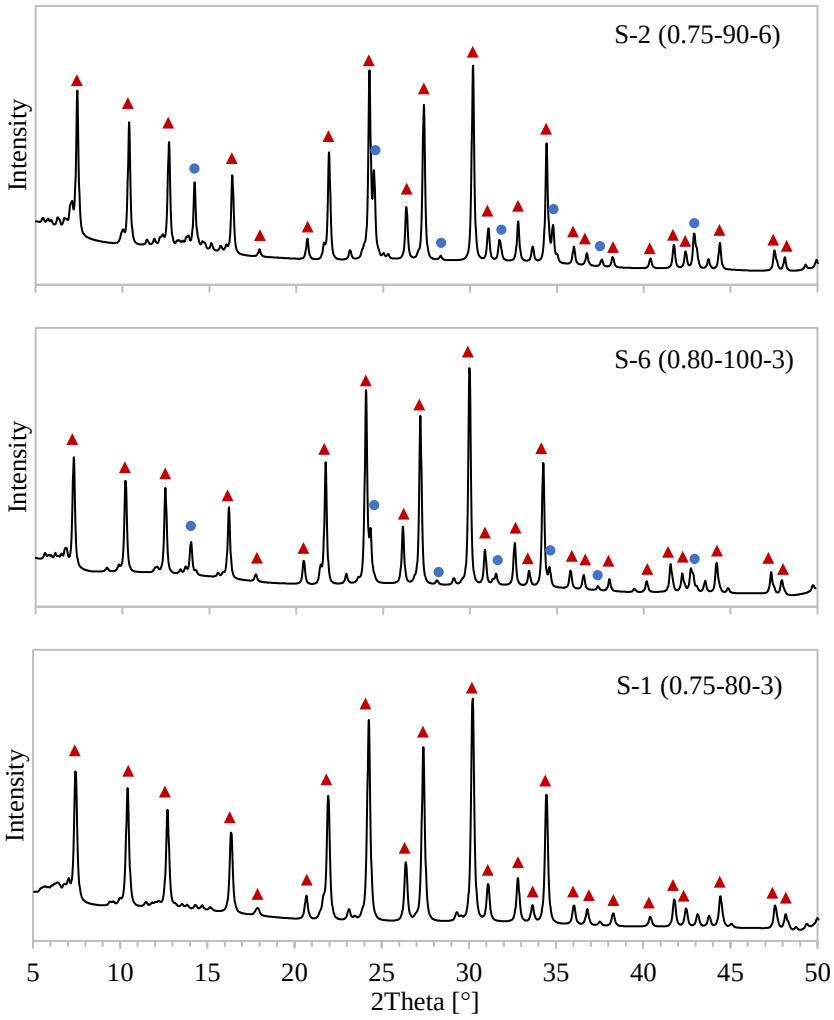


Fig. 7. XRD patterns of the representative synthetic products S-# (i-j-k) (# is the specimen code, i is Si/Al molar ratio, j is crystallization temperature, and k is reaction time).

Figure 7 shows the XRD patterns of four representative synthetic products. For the synthetic products S-2 (0.75-90-6), S-5 (0.80-90-9) and S-6 (0.80-100-3), both zeolite A and zeolite Hydroxy Sodalite (HS) were observed. The product S-5 (0.80-90-9) showed a higher amount of zeolite HS and a lower amount of zeolite A, whilst the product S-6 (0.80-100-3) showed a lower amount of zeolite HS and a higher amount of zeolite A. It corresponds to their percentages of crystalline water release from these synthetic products. Zeolite HS has channels with a micro-pore size of about 2.3 Å while zeolite A has a micro-pore size of approximately 4.1 Å. The formation of zeolite A is preferable to achieve a high percentage of crystalline water in the SSA derived zeolite (Querol et al. 2002).

For the product S-1 (0.75-80-3), their XRD pattern only showed existence of the zeolite A. The XRD pattern of product S-8 (0.85-90-3) which is similar as that of product S-1 (0.75-80-3) is not presented in this paper. Their percentages of crystalline water release were 18.30% and 18.16%, respectively. In the product synthesized under the optimal crystallization conditions, only zeolite A was detected by the XRD analysis. For the products S-4 (0.80-80-6) and S-7 (0.85-80-9) which had the crystalline water release percentages of 17.20% and 17.03%, respectively, a very small amount of zeolite HS was observed in their XRD patterns.

The developed method of SSA recycling generated zeolite A at the relatively lower crystallization temperature and/or shorter reaction time. Under the relatively higher crystallization temperature and/or longer reaction time, it formed zeolite HS. Ojumu et al. (2016) found that for the synthesis of a pure zeolite A, the crystallization temperature needed to be decreased to 80 ºC and 90 ºC and the reaction time varied between 1.5 h and 3 h. The optimal hydrothermal reaction conditions were found to be 2 h at 90 ºC, whereas from 3 h to 6 h zeolite HS started to form. Tounsi et al. (2009) reported that zeolite was synthesized at 90 ºC and after 3 h of crystallization zeolite HS formed. Khajavi et al. (2010) reported that zeolite HS could be synthesized at different crystallization temperatures (90-140 ºC) for different reaction times (3.5-4 h), whereas synthesis for short time and at low temperature led to the co-formation of zeolites A, X, and P in addition to zeolite HS.

*3.5. SEM characterization of synthetic products*

Figure 8 presents the SEM images of the SSA and representative synthetic products. The SSA was characterized by irregular shapes, a typical particle morphology for the combustion byproducts due to the expansion of gases during heating. The zeolite A synthesized under the optimal crystallization conditions exhibited typical cube-shaped morphology.

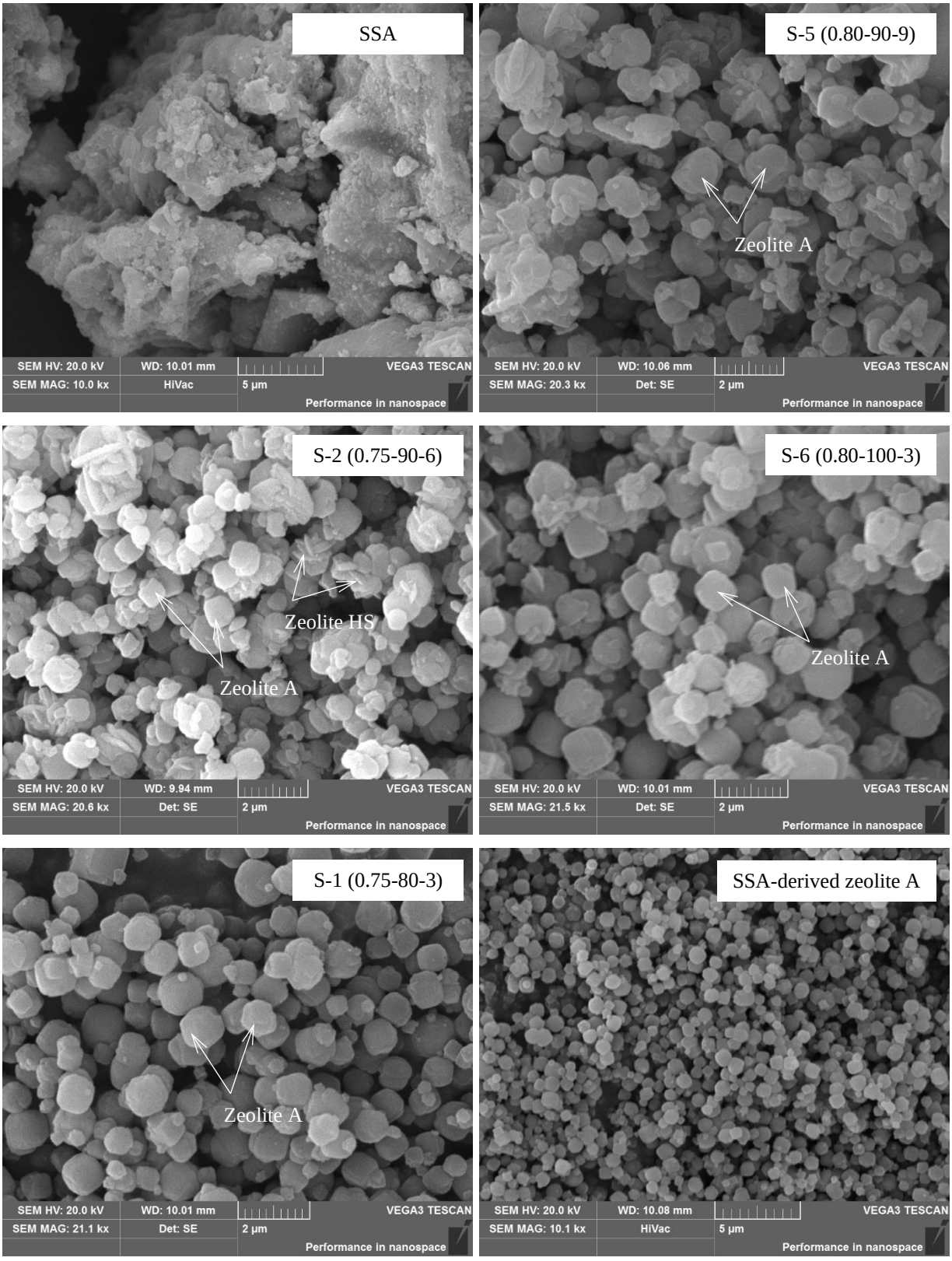


Fig. 8. SEM images of the SSA and representative synthetic products.

Zeolite A and zeolite HS were formed as major crystalline phases in the synthetic products S-2 (0.75-90-6), S-5 (0.80-90-9) and S-6 (0.80-100-3), of which the structures were revealed by the SEM images. In the product S-5 (0.80-90-9), a small amount of the grains with cube-shaped morphology, which were identified as zeolite A, were observed. The SEM image of the product S-2 (0.75-90-6) shows both cube-shaped grains and flaky grains, with similar quantities. In the product S-6 (0.80-100-3), there were a large amount of the cube-shaped grains, representing zeolite HS particles according to the XRD evidence. The similar morphologies of zeolite A and zeolite HS were reported by Tounsi et al. (2009) and Kim and Lee (2009). In the product S-1 (0.75-80-3), only zeolite A particles were observed. Under the optimal crystallization conditions, SSA-derived zeolite A with a high purity was synthesized. These findings indicate that when the crystallization was conducted at the relatively higher temperature and/or longer time, it favors the formation of zeolite HS, which are consistent with the XRD results (Figure 7) as discussed in the previous section.

*3.6. WMA mixtures*

The zeolite A synthesized from SSA under the optimal crystallization conditions was used as an additive to produce WMA mixture. The commercial WMA additive Aspha-Min®, was also applied to produce WMA mixture for comparison. The HMA mixture with the same mixture design was produced as a reference. Figure 9 shows the results of Marshall test of HMA mixture and WMA mixtures with Aspha-Min® and SSA-derived zeolite A. With a decrease of 25 ºC in the production and compaction temperatures, Marshall specimens with average air void contents of 3.73% and 3.59% were successfully produced for the WMA mixtures with Aspha-Min® and the SSA-derived zeolite A, respectively. In comparison, the average air void content of HMA Marshall specimens was 3.23%. All of them meet the requirement for the air void content, which is between 3.0% and 5.0%.

In the Marshall design method, the asphalt mixture also needs to meet requirements for mechanical properties such as the Marshall stability and flow number. It was found that the average Marshall stabilities for HMA mixture and WMA mixtures with Aspha-Min® and SSA-derived zeolite A were 13.97 kN, 11.16 kN, and 11.27 kN, respectively. The flow numbers for HMA mixture and WMA mixtures with Aspha-Min® and synthetic zeolite A were 2.46 mm, 2.42 mm, and 2.70 mm, respectively. Both the HMA mixture and WMA mixtures with Aspha-Min® and synthetic zeolite

A complied with the acceptance requirements for Marshall stability and flow number (i.e., larger than 10 kN and less than 4 mm). Thus, SSA-derived zeolite A product can be an alternative to commercial WMA additives with comparable performance, which illustrates a sustainable and cleaner production approach.

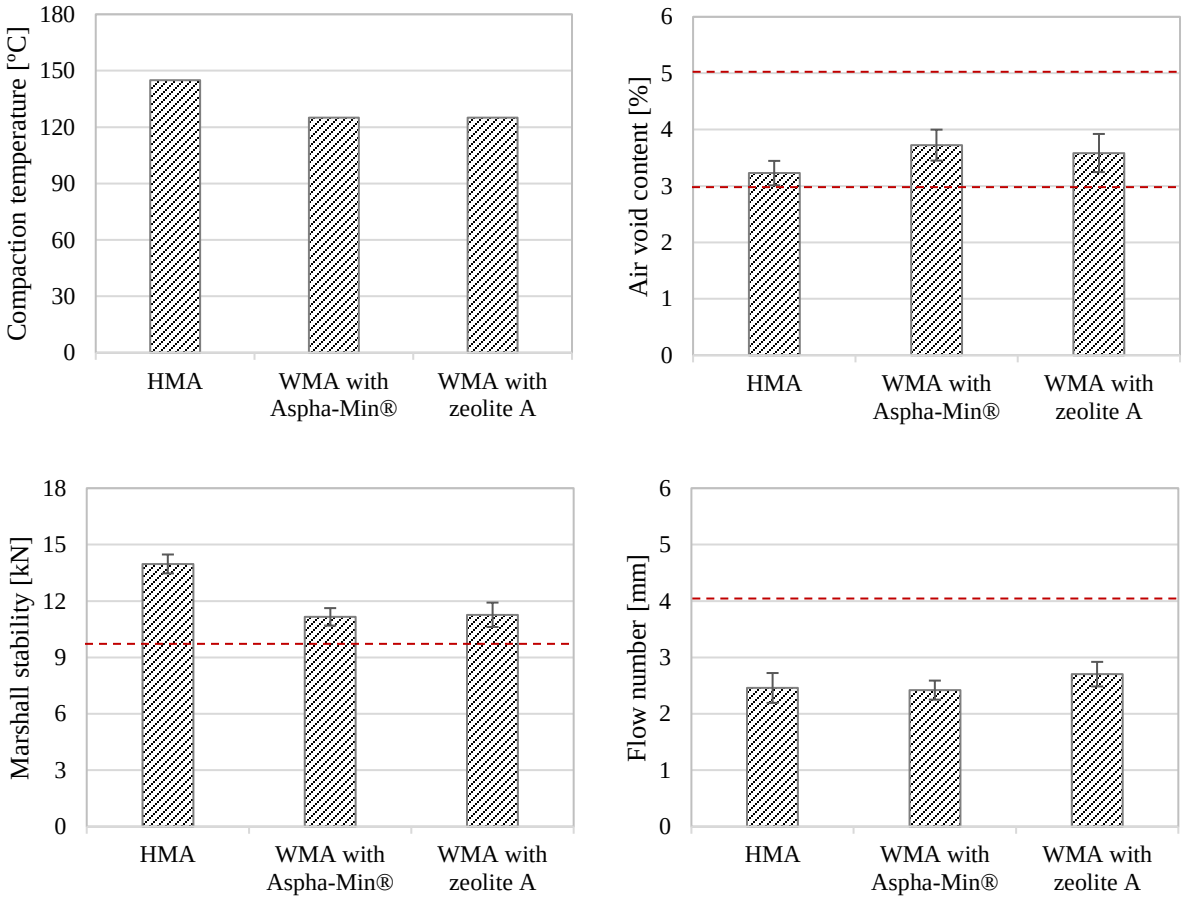


Fig. 9. Marshall test results of the HMA mixture and WMA mixtures with Aspha-Min® and synthetic zeolite A.

## 4. Conclusions

SSA from sludge treatment facilities contains large percentages of silicon dioxide and aluminium oxide which can be used as source materials for the hydrothermal synthesis of zeolites. The economic and environmental concerns generated by the conventional landfill disposal of SSA can be addressed by converting SSA to zeolite A and applying it as a WMA additive. In this research, zeolite products were produced from SSA through the process of alkaline fusion followed by

hydrothermal reaction. The alkaline fusion with a NaOH/SSA mass ratio of 1.15 at 500 ºC for 1 h is the optimal condition for activing SSA for hydrothermal synthesis. In the hydrothermal reaction process, the NaOH solution with a concentration of 2.5 mol/L maximizes dissolution of Si and Al from the fused product at 65 ºC for 3 h. A pure zeolite A can be synthesized under the optimal crystallization conditions, i.e., a Si/Al molar ratio of 0.80, a crystallization temperature of 80 ºC and a reaction time of 3 h. Our developed SSA recycling method tends to generate zeolite A when the crystallization is conducted at the relatively lower crystallization temperature and/or shorter reaction time. Under the condition of relatively higher crystallization temperature and/or longer reaction time, it favors the crystallization of zeolite HS. By adding the zeolite A synthesized from the SSA as a WMA additive, WMA mixture can be successfully produced with a reduction of 25 ºC for both mixing and compaction temperatures. The SSA-derived zeolite A complies with all requirements prescribed by technical standards and it presents a new and cleaner production method of WMA additive for environmental benefits.

**Acknowledgements**

This research was supported by the Hong Kong Environment and Conservation Fund (grant number ECF61/2015).

**References**

Afzal, M., Yasmeen, G., Saleem, M., Butt, P.K., Khattak, A.K., Afzal, J., 2000. TG and DTA study of the thermal dehydration of metal-exchanged zeolite-4A samples. Journal of Thermal Analysis and Calorimetry 62, 721-727.

Al-Qadi, I., Leng, Z., Baek, J., Wang, H., Doyen, M., and Gillen, S., 2012. Short-term performance of plant-mixed warm stone mastic asphalt. Journal of Transportation Research Record, TRR2306, 86-94.

ASTM D3203, 2011. Standard test method for percent air voids in compacted dense and open bituminous paving mixtures. American Section of the International Association for Testing Materials.

ASTM D6927, 2015. Standard test method for Marshall stability and flow of asphalt mixtures. American Section of the International Association for Testing Materials.

403 Bukhari, S.S., Behin, H., Kazemian, H., Rohani, S., 2015. Conversion of coal fly ash to zeolite
404 utilizing microwave and ultrasound energies: A review. Fuel 140, 250-266.
405 Cardoso, A.M., Horn, M.B., Ferret, L.S., Azevedo, C.M.N., Pires, M., 2015. Integrated synthesis
406 of zeolites 4A and Na-P1 using coal fly ash for application in the formulation of detergents and
407 swine wastewater treatment. Journal of Hazardous Materials 287, 69-77.
408 Cieslik, B., Konieczka, P., 2017. A review of phosphorus recovery methods at various steps of
409 wastewater treatment and sewage sludge management. The concept of "no solid waste generation"
410 and analytical methods. Journal of Cleaner Production 142, 1728-1740.
411 Cyr, M., Coutand, M., Clastres, P., 2007. Technological and environmental behavior of sewage
412 sludge ash (SSA) in cement-based materials. Cement and Concrete Research 37, 1278-1289.
413 Dubravský, M., Mandula, J., 2015. Modified asphalt binder with natural zeolite for warm mix
414 asphalt. Journal of Civil Engineering 10, https://doi.org/10.2478/sspjce-2015-0018.
415 Georgiev, D., Bogdanov, B., Angelova, K., Markovska, I., Hristov, Y., 2009. Synthetic zeolites –
416 structure, classification, current trends in zeolite synthesis review. International Science
417 Conference "Economics and Society development on the Base of Knowledge", Stara Zagora,
418 Bulgaria.
419 HK EPD, 2017. Monitoring of solid waste in Hong Kong - waster statistics for 2015.
420 Environmental Protection Department, Hong Kong SAR Government.
421 Hollman, G.G., Steenbruggen, G., Janssen-Jurkovicova, M., 1999. A two-step process for the
422 synthesis of zeolites from coal fly ash. Fuel 78, 1225-1230.
423 Hossain, Z., O'Rear, E., Cross, S., Lewis, S., 2009. Evaluation of the use of warm mix asphalt as
424 a viable paving material in the United States. Final Report, Cooperative Agreement: DTFH61-06-
425 H-00044: Task 3, Federal Highway Administration, McLean, Virginia.
426 Hurley, G.C., Prowell, B.D., 2005. Evaluation of aspha-min® zeolite for use in warm mix asphalt.
427 NCAT Report 05-04, National Center for Asphalt Technology, Alabama, United States.
428 Inada, M., Eguchi, Y., Enomoto, N., Hojo, J., 2005. Synthesis of zeolite from coal fly ashes with
429 difference silica-alumina composition. Fuel 84, 299-304.
430 Joseph, J., Pignatiello, J.R., 1988. An overview of the strategy and tactics of Taguchi. IIE
431 Transactions 20(3), 247-254.
432 Khajavi, S., Sartipi, S., Gascon, J., Jansen, J.C., Kapteijn, F., 2010. Thermostability of hydroxy
433 sodalite in view of membrane applications. Microporous and Mesoporous Materials 132, 510-517.

Kim, J.K., Lee, H.D., 2009. Effects of step change of heating source on synthesis of zeolite 4A from coal fly ash. Journal of Industrial and Engineering Chemistry 15, 736-742.

Lam, C., Lee, P., Hsu, S., 2016. Eco-efficiency analysis of sludge treatment scenarios in urban cities: the case of Hong Kong. Journal of Cleaner Production 112, 3028-3039.

Latosińska, J., 2016. Zeolitization of sewage sludge ash with a fusion method. Journal of Ecological Engineering 17:5, 138-146.

Leng, Z., Gamez, A., Al-Qadi, I., 2014. Mechanical property characterization of warm-mix asphalt prepared with chemical additive. Journal of Materials in Civil Engineering 26:2, 304-311.

Molina, A., Poole, C., 2004. A comparative study using two methods to produce zeolites from fly ash. Minerals Engineering 17, 167-173.

Murayama, N., Yamamoto, H., Shibata, J., 2002. Mechanism of zeolite synthesis from coal fly ash by alkali hydrothermal reaction. Int. J. Miner. Process. 64, 1-17.

Musyoka, N.M., Petrik, L., Hums, E., 2012. Synthesis of zeolite A, X and P from a South African coal fly ash. Advanced Materials Research 512-515, 1757-1762.

Musyoka, N.M., Petrik, L.F., Hums, E., Kuhnt, A., Schwieger, W., 2015. Thermal stability studies of zeolites A and X synthesized from South African coal fly ash. Research on Chemical Intermediates 41:2, 575-582.

Ojumu, T.V., Plessis, P.W.D., Petrik, L.F., 2016. Synthesis of zeolite A from coal fly ash using ultrasonic treatment – A replacement for fusion step. Ultrasonics Sonochemistry 31, 342-349.

Querol, X., Moreno, N., Umana, J.C., Alastuey, A., Hernandez, E., Lopez-Soler, A., Plana, F., 2002. Synthesis of zeolites from coal fly ash: an overview. International Journal of Coal Geology 50, 413-423.

Rao, R.S., Kumar, C.G., Prakasham, R.S., Hobbs, P.J., 2008. The Taguchi methodology as a statistical tool for biotechnological applications: A critical appraisal. Biotechnol. J. 3, 510-523.

Rodriguez-Alloza, A., Malik, A., Lenzen, M., Gallego, J., 2015. Hybrid input-output life cycle assessment of warm mix asphalt mixtures. Journal of Cleaner Production 90, 171-182.

Rios, C.A., Williams, C.D., Fullen, M.A., 2009. Nucleation and growth history of zeolite LTA synthesized from kaolinite by two different methods. Applied Clay Science 42, 446-454.

Rubio, M.C., Martinez, G., Baena, L., Moreno, F., 2012. Warm mix asphalt: an overview. Journal of Cleaner Production 24, 76-84.

Sanchez-Alonso, E., Vega-Zamanillo, A., Castro-Fresno, D., DelRio-Prat, M., 2011. Evaluation of compactability and mechanical properties of bituminous mixes with warm additives. Construction and Building Materials 25, 2304-2311.

Sengoz, B., Topal, A., Gorkem, C., 2013. Evaluation of natural zeolite as warm mix asphalt additive and its comparison with other warm mix additives. Construction and Building Materials 43, 242-252.

Smol, M., Kulczycka, J., Henclik, A., Gorazda, K., Wzorek, Z., 2015. The possible use of sewage sludge ash (SSA) in the construction industry as a way towards a circular economy. Journal of Cleaner Production 95, 45-54.

Somerset, V.S., Petrik, L.F., White, R.A., Klink, M.J., Key, D., Iwuoha, E.I., 2005. Alkaline hydrothermal zeolites synthesized from high SiO2 and Al2O3 co-disposal fly ash filtrates. Fuel 84, 2324-2329.

Stimilli, A., Virgili, A., Canestrari, F., 2017. Warm recycling of flexible pavements: effectiveness of warm mix asphalt additives on modified bitumen and mixture performance. Journal of Cleaner Production 156, 911-922.

Tanaka, H., Fujii, A., Fujimoto, S., Tanaka, Y., 2008. Microwave-assisted two-step process for the synthesis of a single-phase Na-A zeolite from coal fly ash. Advanced Powder Technology 19, 83-94.

Tang, Y., Shih, K., 2014. Beneficial use of aluminium and iron components of sludge incineration residues in ceramic materials. HKIE Transactions 21:4, 223-231.

Topal, A., Sengoz, B., Kok, B.V., Yilmaz, M., Dokandari, P.A., Oner, J., Kaya, D., 2014. Evaluation of mixture characteristics of warm mix asphalt involving natural and synthetic zeolite additives. Construction and Building Materials 57, 38-44.

Tounsi, H., Mseddi, S., Djemel, S., 2009. Preparation and characterization of Na-LTA zeolite from Tunisian sand and aluminum scrap. Physics Procedia 2, 1065-1074.

Vidal, R., Moliner, E., Martínez, G., Rubio, M.C., 2013. Life cycle assessment of hot mix asphalt and zeolite-based warm mix asphalt with reclaimed asphalt pavement. Resources, Conservation and Recycling 74, 101-114.

Woszuk, A., Franus, W., 2017. A review of the application of zeolite materials in warm mix asphalt technologies. Applied Sciences 7, 293.